

# A NUMERICAL STUDY OF A COMPOSITE SANDWICH PANEL UNDER OBLIQUE IMPACT

Yuan Chen<sup>1,2</sup>, Xu Han<sup>1</sup>, Shujuan Hou<sup>1</sup>, Kunkun Fu<sup>2</sup> and Lin Ye<sup>2</sup>

<sup>1</sup>State Key Laboratory of Advanced Design and Manufacturing for Vehicle Body, Hunan University  
Changsha City 410082, P R China  
Email: [ychen0911@163.com](mailto:ychen0911@163.com), [hanxu@hnu.edu.cn](mailto:hanxu@hnu.edu.cn), [shujuanhou@hnu.edu.cn](mailto:shujuanhou@hnu.edu.cn),  
Web page: <http://www.hnu.edu.cn/>

<sup>2</sup>Centre for Advanced Materials Technology (CAMT), School of Aerospace, Mechanical and  
Mechatronic Engineering, The University of Sydney  
NSW 2006, Australia  
Email: [kunkun.fu@sydney.edu.au](mailto:kunkun.fu@sydney.edu.au), [lin.ye@sydney.edu.au](mailto:lin.ye@sydney.edu.au),  
Web page: <http://sydney.edu.au/camt/>

**Keywords:** Composite sandwich panel; transverse impact; oblique impact; modelling.

## ABSTRACT

Composite sandwich panels have becoming increasingly important in recent years in a wide range of applications. This study develops a numerical model that describes a number of damage mechanisms and deformation behaviours in a composite sandwich panel subjected to transverse impact, addressing elastic-plastic behaviours of the core materials, fibre fracture, matrix micro-cracking and energy absorption in the composite panel. The numerical model is validated by a transverse impact test on a composite panel. The load-displacement relationship of the numerical simulation correlates well with that from the experiment, and the total absorbed energy is well predicted, with an error of -6.5%. Further, to improve understanding of transverse impact obliquities, the model is extended to predict the damage to a composite sandwich panel under oblique impact. The results clearly indicate that the total absorbed energy increases significantly as the impact obliquity increases, an effect attributed to the increased damage area and friction.

## 1 INTRODUCTION

Composite materials and structures have attracted increasingly wide interest in a number of industrial applications. As frequently used structures, composite sandwich panels play an important role in defence against impact and in security protection, due to their high strength and excellent energy absorption capabilities. Furthermore, most damage in composite sandwich panels is caused by dynamic loadings, which exist universally in real-life scenarios. In the study of composite sandwich panels under impact loading, two basic and effective approaches have been used, the experimental technique and the numerical method [1]. Experimental analysis is commonly performed to understand the damage process and failure behaviours of composite sandwich panels. For instance, Herup et al. [2] carried out a drop-weight impact and a pendulum impact test on graphite/epoxy sandwiches with honeycomb cores, and concluded that the difference between static contact and low-velocity impact was more significant for sandwich structures with thicker face sheets. Anderson et al. [3] compared the categories and extent of damage between graphite/epoxy face sheets with honeycomb cores and with foam cores under different low-velocity impacts induced by increasing initial energy. On the other hand, a number of numerical models have been developed to predict the damage characteristics and failure behaviours of composite sandwich panels under impact loading [4-7]. For example, Foo et al. [4] used a 3D numerical model to study the damage responses of composite sandwiches after correlation with experimental results. Shi et al. [5] conducted experiments to obtain the load-displacement curves to verify an established damage model programmed using a user-defined material subroutine. Ivañez et al. [6] calculated and predicted the low-velocity impact response of a composite sandwich beam by implementing Hou failure criteria for the composite face sheets and elastic-plastic theories for the honeycomb core. Chen et al. [7] applied a systematic damage predictive method

considering the damage, evaluation and failure of composite panels with a non-metallic honeycomb core, investigating low-velocity impact responses and failure behaviours both numerically and experimentally.

In practical engineering situations, the direction of impact is usually not just perpendicular to the surface of the panel. Hence, investigation of the oblique impact responses of composite sandwich panels is necessary and timely, to develop better understanding of the corresponding responses in scenarios that are more representative of practice. Although Ivañez et al. [8] performed experiments on the damage responses of composite sandwich honeycomb structures under oblique low-velocity impact, relevant studies and data are sparse to date.

This work presents a numerical model for simulating the impact behaviours and calculating the responses of a composite sandwich panel made of carbon fibre reinforced epoxy face sheets with a honeycomb core, using a progressive continuum damage method (CDM) and a cohesive zone method (CZM). The numerical results are validated by experiment and further applied to predict the behaviours and responses of the panel under low-velocity impact with diverse obliquity.

## 2 NUMERICAL MODELS

### 2.1 Numerical simulation

The finite element method is widely used to study the responses of sandwich structures [9], and in our work, the numerical model was established using the commercial code in Abaqus [10]. First, the impactor was modelled rigidly. Second, the boundary conditions including the geometry and load were built according to the experimental set-up. Lastly, the composite sandwich panel was established considering three parts: the composite face sheets, the core and the adhesive.

The composite face sheets were fabricated by T300 plain weave materials with epoxy resin, and contained four layers as the basis of the plies [(45/-45), (0/90), (90/0), (-45/45)] with each layer 0.22 mm in thickness. The basic properties of the T300 plain weave epoxy face sheets are provided in Table 1.

Description	Variable	Value
Density ( $\text{kg/m}^3$ )	$\rho$	1570.5
Fibre volume (%)	$V$	56
Longitudinal Young's modulus (GPa)	$E_{11}$	55.8
Transversal Young's modulus (GPa)	$E_{22}$	55.8
Principal Poisson's ratio (MPa)	$\nu_{12}$	0.06
Shear modulus (MPa)	$G_{12}$	3650
Longitudinal tensile and compressive strength (MPa)	$X_{1+}=X_{2+}$	630
Transverse tensile and compressive strength (MPa)	$X_{1-}=X_{2-}$	550
In-plane shear strength (MPa)	$S_{12}$	100
Inter-laminar normal strength (MPa)	$t_n^0$	62.3
Inter-laminar shear strength (MPa)	$t_s^0 = t_t^0$	92.3
Mode I fracture toughness ( $\text{KJ/m}^2$ )	$G_I^C$	0.519
Mode II fracture toughness ( $\text{KJ/m}^2$ )	$G_{II}^C = G_{III}^C$	2.416

Table 1: Properties of T300 plain weave epoxy composite material [7].

To simulate the damage and failure of the composite face sheets, the CDM was applied to reflect the degradation of the material stiffness matrix. The fibre directions of the woven fabric composite materials were assumed to be orthogonal linear elastic. Then, the constitutive stress-strain relations could be formulated as follows [11]:

$$\begin{Bmatrix} \sigma_{11} \\ \sigma_{22} \\ \sigma_{12} \end{Bmatrix} = \frac{1}{D} \begin{bmatrix} (1-d_1)E_1 & (1-d_1)(1-d_2)E_1\nu_{21} & 0 \\ (1-d_1)(1-d_2)E_2\nu_{12} & (1-d_2)E_2 & 0 \\ 0 & 0 & 2(1-d_{12})DG_{12} \end{bmatrix} \begin{Bmatrix} \varepsilon_{11} \\ \varepsilon_{22} \\ \varepsilon_{12}^{el} \end{Bmatrix} \quad (1)$$

where  $\sigma_{11}$ ,  $\sigma_{22}$  and  $\sigma_{12}$  are the stresses and  $\varepsilon_{11}$ ,  $\varepsilon_{22}$  and  $\varepsilon_{12}^{el}$  are the elastic strains, respectively.  $D=1-(1-d_1)(1-d_2)\nu_{12}\nu_{21}$ ,  $d_1$  and  $d_2$  are the damage variables,  $d_{12}$  reflects the current shear damage state taking into account the matrix micro-cracking; the damage variables depict the degradation within the material;  $E_1$  and  $E_2$  are Young's moduli along the intersecting fibre directions, respectively,  $G_{12}$  is the in-plane shear modulus,  $\nu_{12}$  and  $\nu_{21}$  are Poisson ratios. In this work, the damage variables were calculated based on the stress state in the fibre directions as

$$d_i = d_{i+} \frac{\langle \sigma_{ii} \rangle}{|\sigma_{ii}|} + d_{i-} \frac{\langle -\sigma_{ii} \rangle}{|\sigma_{ii}|}, i=1, 2 \quad (2)$$

where  $d_{i+}$ ,  $d_{i-}$  and  $d_{12}$  are the damage variables that are assumed as a function of the corresponding effective stress. Prior to calculating the damage behaviours with regard to the fibre fracture and matrix micro-cracking with plasticity, the initiation failure criteria could be given directly as [12]

$$\varphi_{i+} = \frac{\tilde{\sigma}_{i+}}{X_{i+}} \quad \varphi_{i-} = \frac{\tilde{\sigma}_{i-}}{X_{i-}} \quad \varphi_{12} = \frac{\tilde{\sigma}_{12}}{S_{12}} \quad (3)$$

In Equation (3),  $X_{i+}$  and  $X_{i-}$  are the tensile or compressive strengths, respectively, and  $S_{12}$  is the shear strength; when the initiation index  $\varphi_{i+}$ ,  $\varphi_{i-}$ , or  $\varphi_{12}$  is equal to 1 the corresponding damage mode is activated. Subsequently, the damage evaluation is implemented in accordance with [13] by calculating and developing the damage variables.

In the evaluation of shear damage, except for that caused by micro-cracking of the matrix, plasticity should also be taken into account. The plasticity model and hardening law for the damaged materials are

$$F = |\tilde{\sigma}_{12}| - \tilde{\sigma}_0(\bar{\varepsilon}^{pl}) \leq 0 \quad (4)$$

and

$$\tilde{\sigma}_0(\bar{\varepsilon}^{pl}) = \tilde{\sigma}_{y0} + C(\bar{\varepsilon}^{pl})^p \quad (5)$$

where  $\bar{\varepsilon}^{pl}$  is the equivalent plastic strain and  $\tilde{\sigma}_{y0}$  is the effective yield shear stress,  $C$  and  $p$  are hardening parameters.

During the calculation, structural elements would be deleted if the failure criteria were met. At the same time, in order to remove the elements excessing of severely distortion which might abort the calculation, another element deletion was set as advised in reference [8].

With regard to the interface failure of delamination, the CZM approach was implemented by adopting a damage initiation criterion and a damage evaluation law, to predict both inter-laminar and adhesive damage and failure. The traction-separation method for damage initiation was expressed as [10]

$$\left\{ \frac{\langle t_n \rangle}{t_n^0} \right\}^2 + \left\{ \frac{\langle t_s \rangle}{t_s^0} \right\}^2 + \left\{ \frac{\langle t_t \rangle}{t_t^0} \right\}^2 = 1 \quad (6)$$

In the above,  $t_i$  ( $i=n, s, t$ ) denote the traction stress vector and  $t_i^0$  ( $i=n, s, t$ ) denote respectively the normal and shear strengths. By the Benzeggagh-Kenane fracture criterion [13], the mixed-mode for evaluation based on energy dissipation could be calculated as

$$G_n^C + (G_s^C - G_n^C) \left\{ \frac{G_s}{G_T} \right\}^n = G^C \quad (7)$$

where  $G_S=G_n+G_t$ ,  $G_T=G_n+G_s$ ,  $G_i (i=n, s)$  is the current fracture toughness in the normal and shear directions, respectively;  $G_i^C$  is the corresponding fracture toughness.  $\eta$  is the cohesive property coefficient.

The honeycomb core materials are modelled as isotropic elasto-plastic to improve the efficiency of the calculation [14-16]. The geometric and composite modelling of aramid paper and phenolic resin were proposed and the strain rate effects on the material properties under low-velocity impact have been discussed in previous work [7].

## 2.2 Experimental

To validate the numerical model, low-velocity impact testing was implemented. The specimen made of T300 woven fibre-reinforced epoxy composite materials, as already presented, was plied as [(45/-45), (0/90), (90/0), (-45/45)], and the curing lasted two hours at 177 °C [17]. To suit the clamping size of the drop weight machine, the final specimen was cut using a bandsaw. For the drop weight machine, a hemispherical impactor with the diameter of 12.5 mm was carefully installed at the top. Meanwhile, at the bottom, the margin of the specimen was uniformly clamped by a fixture which spared a circular area for the impact test. During testing, the velocity, the plot of impact force and the deflection were recorded by a data collection computer, and the initial velocity gathered by the collection system was 4.59 m/s.

## 3 RESULTS AND DISCUSSION

After the numerical simulation and experimental validation of the composite sandwich panel under low-velocity impact, the basic damage and failure patterns and responses could be obtained and analysed directly. Also, when the numerical method had been verified, this model was further utilised to predict and investigate the damage processes and the mechanical responses of the composite sandwich panels associated with impact obliquity.

### 3.1 Comparison of numerical and experimental results

From Figure 1, it can be seen that the load-displacement curve obtained by the numerical calculation correlates well with the experimental result. The first peak force is 1160.72 N of the numerical result, which is just 0.35% error compared to the experimental result. Although the errors of the second peak force and the low valley are slightly above 10%, they would not affect the predictive accuracy of the total energy absorption, being -6.5%. Therefore, the numerical model was deemed capable of predicting the responses of the composite sandwich panel under transverse low-velocity impact.

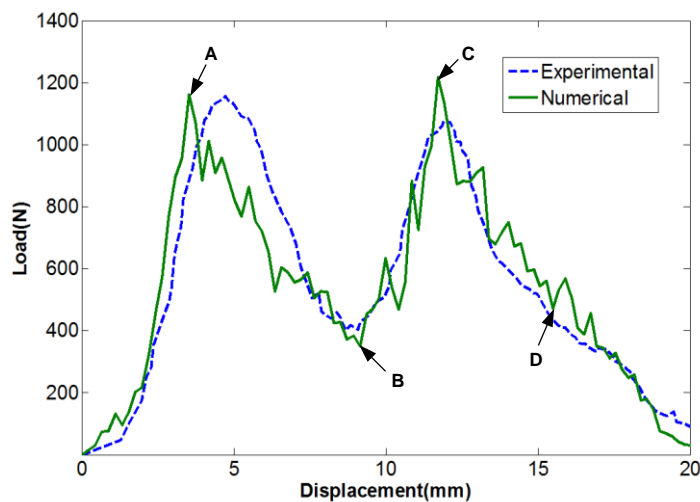


Figure 1: Comparison of the load-displacement curves between the experimental and numerical results under normal impact.

For better realization of the damage process of the composite sandwich panel under impact, a cross-sectional view is presented in Figure 2 (in which the four positions are related to the points in Figure 1). At point A, the first maximum force involves intensive stresses at and around the centre of the contact surface between the impactor and the panel, also producing a number of compressions and shearing forces along the interface between the front panel and the honeycomb core. Subsequently, the impact force descends all the way to the minimum at point B before climbing up to the second peak at point C. Finally, the entire panel is penetrated at point D, where intensive stresses surround the crushed hole in contact with the impactor surface.

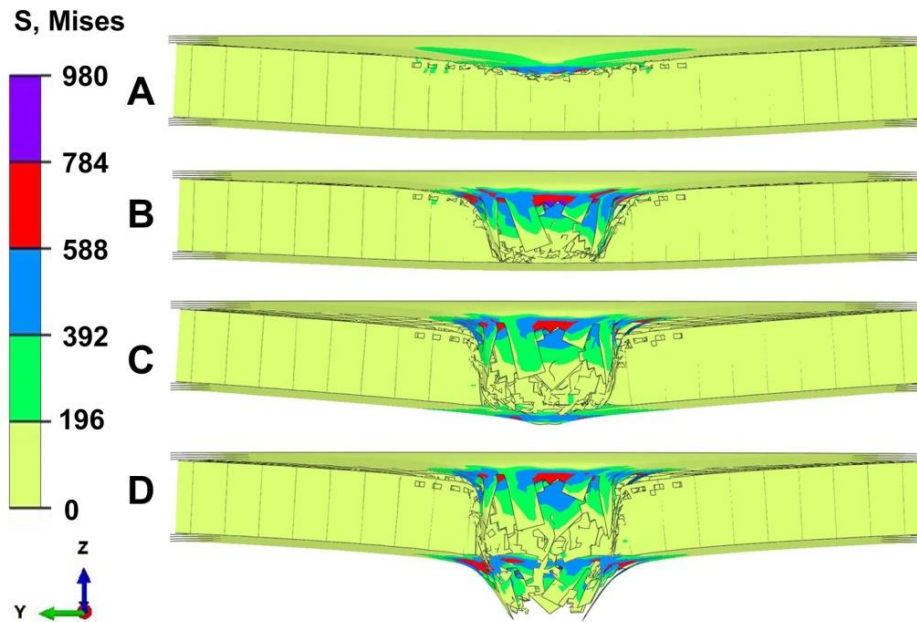


Figure 2: Cross-sectional view of damage process of composite sandwich panel under normal impact.

When the damage zones as shown in Figure 3 are compared, it is evident that the damage pattern (numerical) of the front panel is almost the same as the experimental damage pattern, with a circular penetration hole of the same size as the impactor. As described previously, the intense stresses are mainly concentrated around the penetration hole, particularly in the sections where the cracks end. At the back of the panel, the damage zone is also predicted well by the proposed numerical method. Four almost symmetrical triangles are pulled out from the back panel surface, phenomena which are mostly attributed to the local squeezing forces from the impactor. It can also be seen that cracks propagate along the intersecting fibre directions throughout the whole back panel. After all comparisons and analyses were completed, the numerical model of the composite sandwich panel under low-velocity impact was deemed to predict accurately and thus could be used for subsequent investigations.

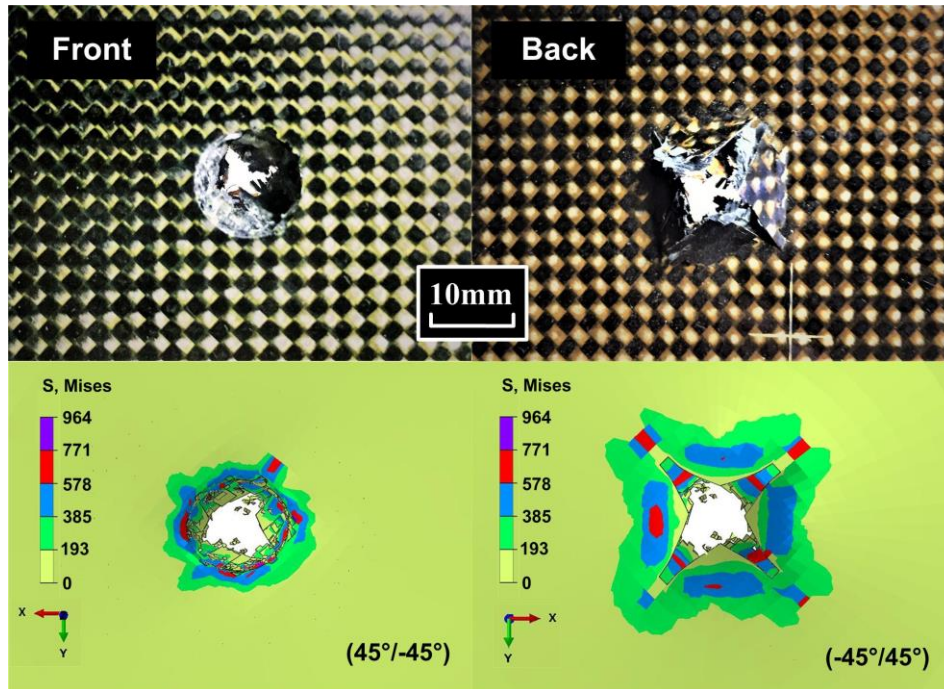


Figure 3: Comparison of the damage patterns of the front and back panels between experimental (upper) and numerical results (bottom).

### 3.2 Numerical study of impact obliquity

As already stated, the effects of impact obliquity on composite sandwich panels have seldom been reported, but this knowledge is quite important. Hence, oblique impacts at angles of  $30^\circ$ ,  $45^\circ$ ,  $60^\circ$ ,  $75^\circ$  and  $90^\circ$  were implemented using the validated model, to study the impact responses and behaviours of the composite sandwich panel. In Figure 4, the selected positions of the panel under different impact angles were acquired at the moment when the impactor protruded from the back panel surface by its radius ( $12.5/2=6.25$  mm), and the impact angles were defined as the angular value between the centre line of the impactor and the original front surface of the panel. As Figure 4 depicts, it is evident that the magnitudes of the stresses of the composite sandwich panel fluctuate insignificantly under different impact angles, and this phenomenon is strongly related to the same impact velocity and the unchanged structures and materials of the composite sandwich panel. However, the damage zones increase significantly in size as the impact angle decreases. In particular, both the debonding between the composite panels and the honeycomb cores and the inter-laminar delamination clearly become more noticeable as the impact angle reduces.

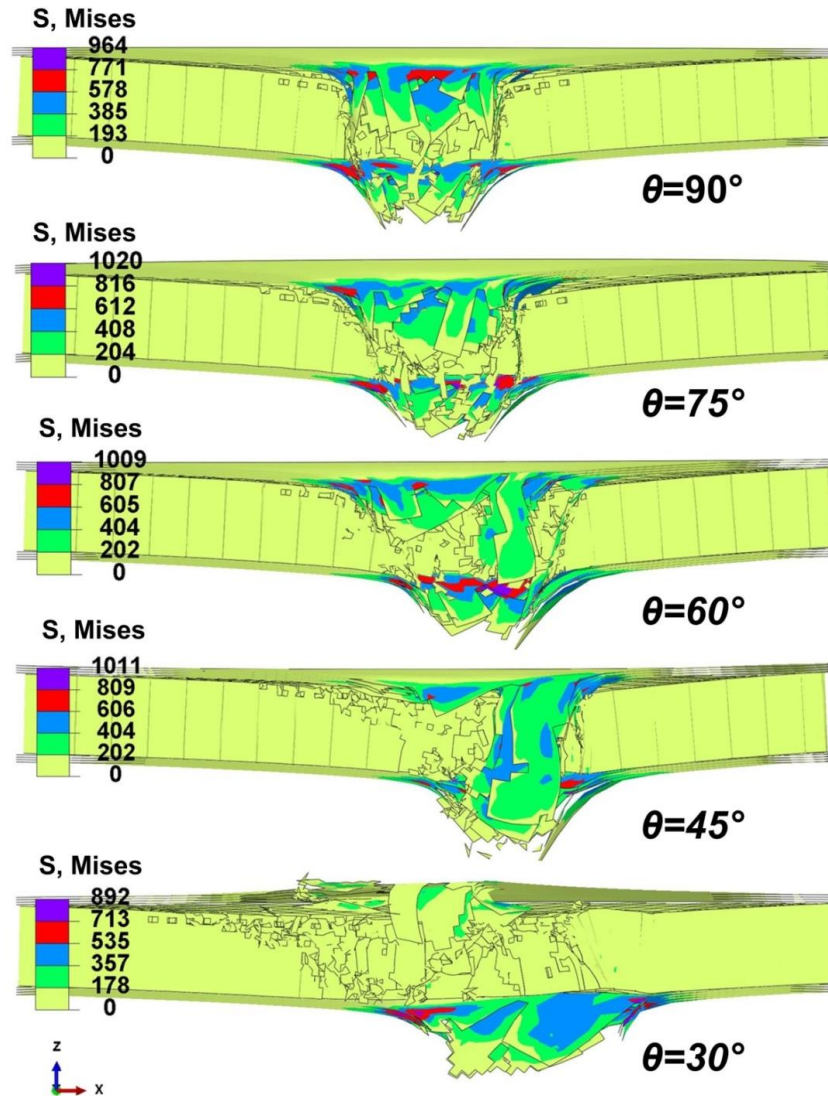


Figure 4: Cross-sectional views of damage patterns of the composite sandwich panel under different impact angles.

Figure 5 presents the load-displacement curves of the composite sandwich panel under different impact angles. It is apparent that the displacement caused by the decreasing impact angles increases, and the timing of both peak and low loads is postponed as the angle decreases. Hence, the total energy absorption is enhanced along with the decreased angular value of the impact. It is worth noting that the energy absorption of the composite sandwich panel under the  $30^\circ$  impact angle is nearly 130% greater than that of the normal impact. The massive increase in the total absorbed energy is basically attributable to the increased damage area of the panel (damage of both composite skin and honeycomb core), associated with longer contact and much greater friction throughout the whole impact system and process. It is also found that the maximum force appears at the oblique impact of  $45^\circ$ , and the first peak force remains at almost the same level while the obliquity changes.

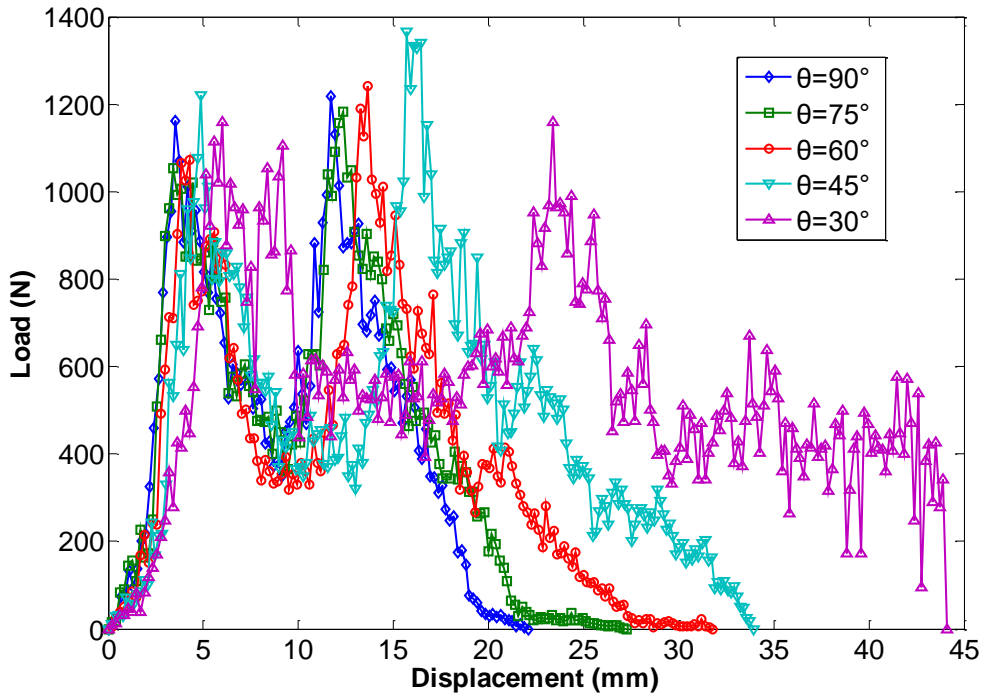


Figure 5: Comparison of load-displacement curves of the composite sandwich panel under different impact angles.

#### 4 CONCLUSIONS

In this study we sought to analyse the effects of low-velocity impact obliquity on the damage and failure responses and behaviours of a composite sandwich panel. First, a numerical model was developed to address the damage and failure of the composite sandwich panel, including progressive continuum damage of the composite skins, elastic-plastic damage of the honeycomb core, and delamination. Second, the numerical model was validated by drop weight testing and, after comprehensive comparisons, it was concluded that the numerical model was capable of predicting the total absorbed energy effectively, with an error of only -6.5% in comparisons with the experimental results. Third, low-velocity oblique impacts were imposed on the composite sandwich panel at different angles, using the validated numerical model. The results indicated that the total absorbed energy increased rapidly with stepwise increasing obliquity of impact. In particular, below a  $30^\circ$  impact angle, the energy absorption of the composite sandwich panel was nearly 1.3 times greater than that of the normal impact. The increasing energy absorption capability was essentially attributed to the increased damage area of the composite sandwich panel and to longer contact with much more friction in the entire impact process.

#### ACKNOWLEDGEMENTS

Financial support from the National Natural Science Foundation of China (11572122, 11372106) is gratefully acknowledged. Moreover, the Joint Centre for Intelligent New Energy Vehicles is also gratefully acknowledged. The first author is also grateful for the support of the China Scholarship Council (CSC) and the School of Aerospace, Mechanical and Mechatronic Engineering, The University of Sydney.

## REFERENCES

- [1] T. Besant, G.A.O. Davies, D. Hitchings, Finite element modelling of low velocity impact of composite sandwich panels, *Composites Part A: Applied Science and Manufacturing*, **32**, 2001, pp.1189-96 (doi: [10.1016/S1359-835X\(01\)00084-7](https://doi.org/10.1016/S1359-835X(01)00084-7)).
- [2] E.J. Herup, A.N. Palazotto, Low-velocity impact damage initiation in graphite/epoxy/nomex honeycomb-sandwich plates, *Composites Science and Technology*, **57**, 1997, pp. 1581-98 (doi: [10.1016/S0266-3538\(97\)00089-4](https://doi.org/10.1016/S0266-3538(97)00089-4)).
- [3] T. Anderson, E. Madenci, Experimental investigation of low-velocity impact characteristics of sandwich composites, *Composites Structure*, **50**, 2000, pp. 239-47 (doi: [10.1016/S0263-8223\(00\)00098-2](https://doi.org/10.1016/S0263-8223(00)00098-2)).
- [4] C.C. Foo, G.B. Chai and L.K. Seah, A model to predict low-velocity impact response and damage in sandwich composites, *Composites Science and Technology*, **68**, 2008, pp. 1348-1356 (doi: [10.1016/j.compscitech.2007.12.007](https://doi.org/10.1016/j.compscitech.2007.12.007)).
- [5] Y. Shi, T. Swait, C. Soutis, Modelling damage evolution in composite laminates subjected to low velocity impact, *Composites Structure*, **94**, 2012, pp. 2902-13 (doi: [10.1016/j.compstruct.2012.03.039](https://doi.org/10.1016/j.compstruct.2012.03.039)).
- [6] I. Ivañez, S. Sanchez-Saez, Numerical modelling of the low-velocity impact response of composite sandwich beams with honeycomb core, *Composites Structure*, **106**, 2013, pp. 716-23 (doi: [10.1016/j.compstruct.2013.07.025](https://doi.org/10.1016/j.compstruct.2013.07.025)).
- [7] Y. Chen, S.J. Hou, K.K. Fu, X. Han, L. Ye, Low-velocity impact response of composite sandwich structures: Modelling and experiment, *Composites Structure*, **168**, 2017, pp. 322-34 (doi: [10.1016/j.compstruct.2017.02.064](https://doi.org/10.1016/j.compstruct.2017.02.064)).
- [8] I. Ivañez, M.M. Moure, S.K. Garcia-Castillo and S. Sanchez-Saez, The oblique impact response of composite sandwich plates, *Composites Structure*, **133**, 2015, pp. 1127-1136 (doi: [10.1016/j.compstruct.2015.08.035](https://doi.org/10.1016/j.compstruct.2015.08.035)).
- [9] S.J. Hou, C.F. Shu, S.Y. Zhao, T.Y. Liu, X. Han and Q. Li, Experimental and numerical studies on multi-layered corrugated sandwich panels under crushing loading, *Composites Structure*, **126**, 2015, pp. 371-385 (doi: [10.1016/j.compstruct.2015.02.039](https://doi.org/10.1016/j.compstruct.2015.02.039)).
- [10] Abaqus® 6.10 Analysis user's manual. Dassault Systèmes; 2010.
- [11] A.F. Johnson, Modelling fabric reinforced composites under impact loads, *Composites Part A: Applied Science and Manufacturing*, **32**, 2001, pp. 1-2 (doi: [10.1016/S1359-835X\(00\)00186-X](https://doi.org/10.1016/S1359-835X(00)00186-X)).
- [12] V.S. Sokolinsky, K.C. Indermuehle and J.A. Hurtado, Numerical simulation of the crushing process of a corrugated composite plate, *Composites Part A: Applied Science and Manufacturing*, **42**, 2011, pp. 1119-1126 (doi: [10.1016/j.compositesa.2011.04.017](https://doi.org/10.1016/j.compositesa.2011.04.017)).
- [13] M. Benzeggagh and M. Kenane, Measurement of mixed-mode delamination fracture toughness of unidirectional glass/epoxy composites with mixed mode bending apparatus, *Composites Science and Technology*, **56**, 1996, pp. 439-449 (doi: [10.1016/0266-3538\(96\)00005-X](https://doi.org/10.1016/0266-3538(96)00005-X)).
- [14] C.T. Sun, Proceedings of the American Society for Composites 17th Technical Conference, CRC Press, Florida, 2002.
- [15] M. Giglio, A. Manes and A. Gilioli, Investigations on sandwich core properties through an experimental-numerical approach, *Composites Part A: Applied Science and Manufacturing*, **43**, 2012, pp. 361-374 (doi: [10.1016/j.compositesb.2011.08.016](https://doi.org/10.1016/j.compositesb.2011.08.016)).
- [16] R. Seemann, D. Krause, Numerical modeling of nomex honeycomb cores for detailed analysis of sandwich panel joints, 11th World Congress on Computational Mechanics (WCCM XI), 2014.
- [17] S. Mustapha, L. Ye, D. Wang and Y. Lu, Assessment of debonding in sandwich CF/EP composite beams using A0 Lamb wave at low frequency, *Composites Structure*, **93**, 2011, pp. 483-491 (doi: [10.1016/j.compstruct.2010.08.032](https://doi.org/10.1016/j.compstruct.2010.08.032)).